

Supporting Information

Modulating electronic structure of Ru by self-reconstructed MOF-NiFeOOH heterointerface for improved electrocatalytic water splitting

Yingkai Guan^a, Tingting Liu^a, Yuanyuan Wu^a, Chunwei Yang^b, Bo Liu^{a,c}, Bo Hu^a, Wei Jiang^{a,b,c,*}, Chunbo Liu^{b,*}, Guangbo Che^{d,*}

^a Key Laboratory of Preparation and Application of Environmental Friendly Materials (Jilin Normal University), Ministry of Education, Changchun 130103, P. R. China.

^b Jilin Joint Technology Innovation Laboratory of Developing and Utilizing Materials of Reducing Pollution and Carbon Emissions, College of Engineering, Jilin Normal University, Siping, 136000, P. R. China.

^c The Joint Laboratory of Intelligent Manufacturing of Energy and Environmental Materials, Jilin Normal University, Siping, 136000, P. R. China.

^d College of Chemistry, Baicheng Normal University, Baicheng, 137018, P. R. China.

**Correspondence author*

E-mail: jiangwjlnu@163.com (Wei Jiang)

E-mail: chunboliu@jlnu.edu.cn (Chunbo Liu)

E-mail: guangboche@jlnu.edu.cn (Guangbo Che)

Fax: +86-434-3290623

Contents

Texts

Text S1. Chemicals reagents.

Text S2. Experimental.

Text S3. Characterization.

Text S4. Electrochemical measurements.

Text S5. Theoretical calculations.

Figures

Fig. S1. SEM images of Ru₁₀/NFF.

Fig. S2. (a-b) SEM images of Ru₅NiFe-MOF/NFF. (c-d) Ru₁₅NiFe-MOF/NFF. (e-f) Ru₂₀NiFe-MOF/NFF.

Fig. S3. (a) EDS images of Ru₅NiFe-MOF/NFF. (b) Ru₁₀NiFe-MOF/NFF. (c) Ru₁₅NiFe-MOF/NFF. (d) Ru₂₀NiFe-MOF/NFF. (e) Ru₁₀NiFeOOH-MOF/NFF.

Fig. S4. XRD images of Ru₁₀NiFe-MOF/NFF、Ru₁₀NiFeOOH-MOF/NFF and NFF.

Fig. S5. Fast scan LSV map of 10 HER tests of Ru₁₀NiFe-MOF/NFF.

Fig. S6. LSV images of Ru₁₀NiFe-MOF/NFF and Ru₁₀NiFeOOH-MOF/NFF.

Fig. S7. (a-g) Cyclic voltammetry of Ru₅NiFeOOH-MOF/NFF, Ru₁₀NiFeOOH-MOF/NFF, Ru₁₅NiFeOOH-MOF/NFF, Ru₂₀NiFeOOH-MOF/NFF, NiFe-MOF/NFF, Pt/C/NFF, NFF at potentials of 0.02-0.1 V.

Fig. S8. ICP images of Ru₁₀NiFeOOH-MOF/NFF.

Table

Table S1. Comparison of atomic percentages of different electrocatalysts.

Texts

Text S1. Chemicals reagents.

All chemicals and reagents were analytically pure and used without further purification. RuCl_3 and 2,5-dihydroxyterephthalic acid (H_4DOBDC) was purchased from Maclean's Reagent Company. N,N-dimethylformamide (DMF) was purchased from Tianjin Tiantai Chemical Co. Ethanol was purchased from Commercial NFF, NF, FF (thickness 1.5 mm) was provided by Longshengbao Co.

Text S2. Experimental

Synthesis of Ru₅NiFe-MOF/NFF, Ru₁₅NiFe-MOF/NFF and Ru₂₀NiFe-MOF/NFF

To provide a comparison, Ru₅NiFe-MOF/NFF, Ru₁₅NiFe-MOF/NFF, and Ru₂₀NiFe-MOF/NFF were constructed using 5, 15, and 20 mg of Ru, respectively, following a similar method as Ru₁₀NiFe-MOF/NFF.

Synthesis of NiFe-MOF/NFF

2, 5-dihydroxyterephthalate H₄DOBDC (0.20 mmol, 40 mg) was dissolved in a mixture of DMF (10 mL), ethanol (0.6 mL) and deionized water (0.6 mL), and transferred to a 40 mL Teflon reactor, in which the pre-treated NFF was placed. After ultrasonic treatment for 30 min, the oven was placed at 105 °C and kept for 12 hours. After the reaction, NiFe-MOF/NFF was obtained.

Text S3. Characterization

The crystalline structure of MOFs was determined using a X-ray diffractometer (XRD, PC2500 JEOL). The morphology of the materials was characterized using scanning electron microscopy (SEM, HITACHI Regulus8100) and transmission electron microscopy (TEM, JEOL JEM-2100). The organic bonds of Ru₁₀NiFeOOH-MOF/NFF were analyzed using Fourier transform infrared (FT-IR, Thermo Scientific Nicolai 4700). Raman spectroscopy (Raman, Horiba HR Evolution) was employed to detect the presence of chemical bonds. The elemental distribution on the electrode surface was determined using energy dispersive X-ray spectrometry (EDS, Oxford UltimMax65). Additionally, the chemical state of the electrode was studied using X-ray photoelectron spectrometer (XPS, Thermal Fisher ESCALAB250 XI) measurements.

Text S4. Electrochemical measurements

Electrochemical investigations were conducted using a PGSTAT-302N electrochemical workstation to test the electrocatalytic performance of electrochemical test in 1 M KOH electrolyte using a three-electrode system with self-supporting electrode (working electrode), carbon rod (counter electrode) and Hg / HgO electrode (reference electrode). For comparison, the commercial RuO₂ loading on the NFF substrate was prepared as follows: Firstly, 5 mg of RuO₂ was dispersed in a mixture of 0.5 mL of ethanol and 0.1 mL of Nafion solution (0.5 wt %). Afterwards, the mixture underwent sonication for 2 h to achieve a uniform catalyst ink, which was then applied to the NFF surface with a loading of 0.2 mg cm⁻². Before the HER investigation started, 10 laps of LSV with a sweep speed of 100 mVs⁻¹ was carried out to activate the electrode. During HER, the LSV curve was recorded with a sweep speed of 1 mV s⁻¹ in a potential range of 0 to -0.4 V vs RHE. In addition, electrochemical impedance spectroscopy (EIS) was performed in the frequency range from 100 kHz to 0.1 Hz.

Text S5. Theoretical calculations.

The Vienna Ab Initio Package (VASP) was employed to perform all the density functional theory (DFT) calculations within the generalized gradient approximation (GGA) using the Perdew, Burke, and Enzerhof (PBE) formulation.^[1-3] The projected augmented wave (PAW) potentials were applied to describe the ionic cores and take valence electrons into account using a plane wave basis set with a kinetic energy cutoff of 450 eV.^[4,5] Partial occupancies of the Kohn–Sham orbitals were allowed using the Gaussian smearing method and a width of 0.05 eV. The electronic energy was considered self-consistent when the energy change was smaller than 10^{-5} eV. A geometry optimization was considered convergent when the force change was smaller than 0.05 eV/Å. Grimme’s DFT-D3 methodology was used to describe the dispersion interactions.^[6] The vacuum spacing perpendicular to the plane of the structure is 20 Å. The Brillouin zone integral utilized the surfaces structures of $2 \times 2 \times 1$ monkhorst pack K-point sampling. The Charge density difference of system: $\Delta\rho = \rho_{\text{total}} - \rho_A - \rho_B$, where ρ_{total} is the charge density of Binding systems, ρ_A and ρ_B is the sub charge density. Finally, the adsorption energies(E_{ads}) were calculated as $E_{\text{ads}} = E_{\text{ad/sub}} - E_{\text{ad}} - E_{\text{sub}}$, where $E_{\text{ad/sub}}$, E_{ad} , and E_{sub} are the total energies of the optimized adsorbate/substrate system, the adsorbate in the structure, and the clean substrate, respectively. The free energy was calculated using the equation:

$$G = E_{\text{ads}} + \text{ZPE} - \text{TS}$$

where G , E_{ads} , ZPE and TS are the free energy, total energy from DFT calculations, zero point energy and entropic contributions, respectively.

Figures

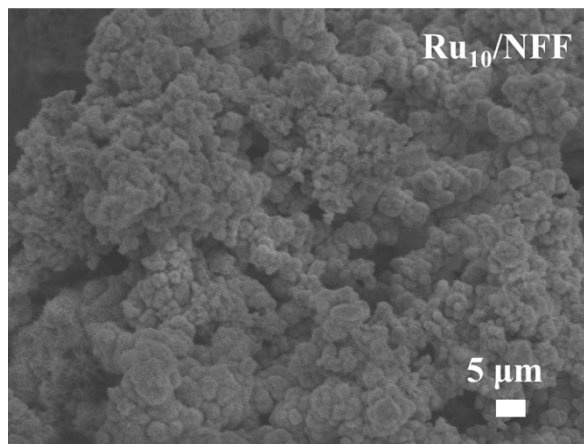


Fig.S1. SEM images of Ru₁₀/NFF.

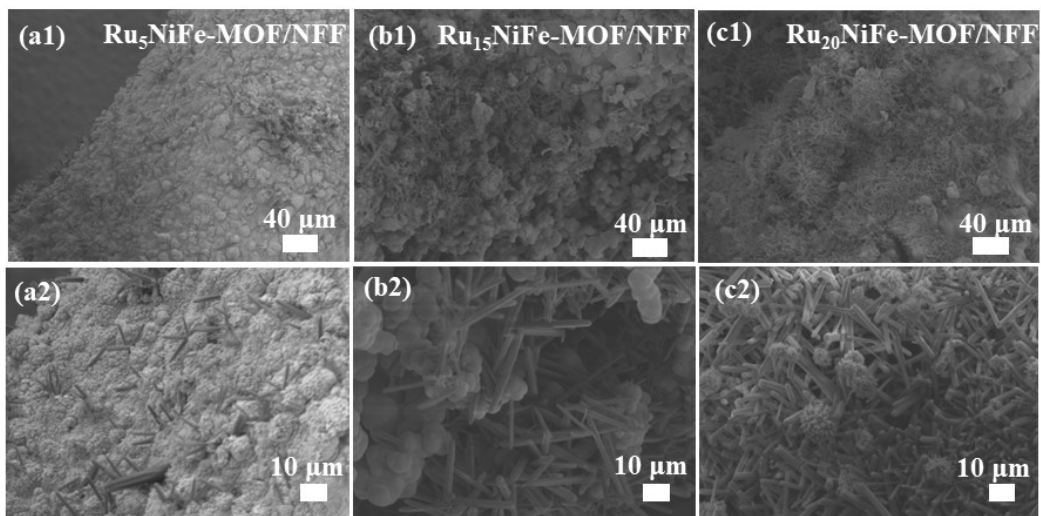


Fig.S2. (a-b) SEM images of Ru₅NiFe-MOF/NFF. (c-d) Ru₁₅NiFe-MOF/NFF. (e-f) Ru₂₀NiFe-MOF/NFF.

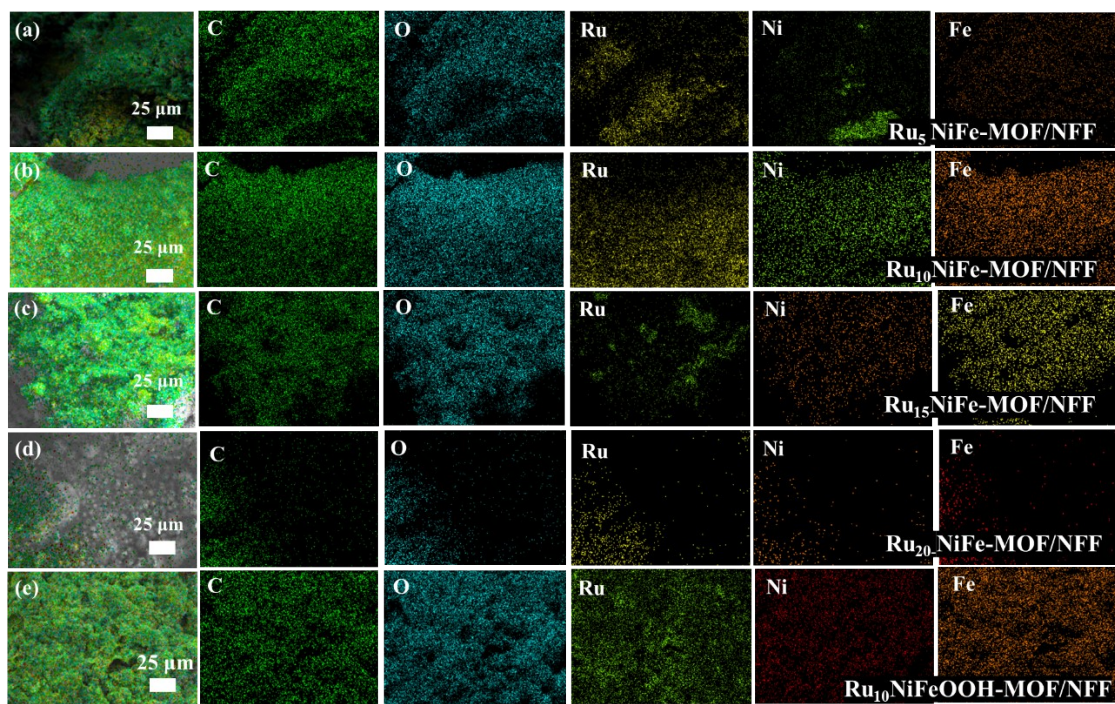


Fig.S3. (a) EDS images of $\text{Ru}_5\text{NiFe-MOF/NFF}$. (b) $\text{Ru}_{10}\text{NiFe-MOF/NFF}$. (c) $\text{Ru}_{15}\text{NiFe-MOF/NFF}$. (d) $\text{Ru}_{20}\text{NiFe-MOF/NFF}$. (e) $\text{Ru}_{10}\text{NiFeOOH-MOF/NFF}$.

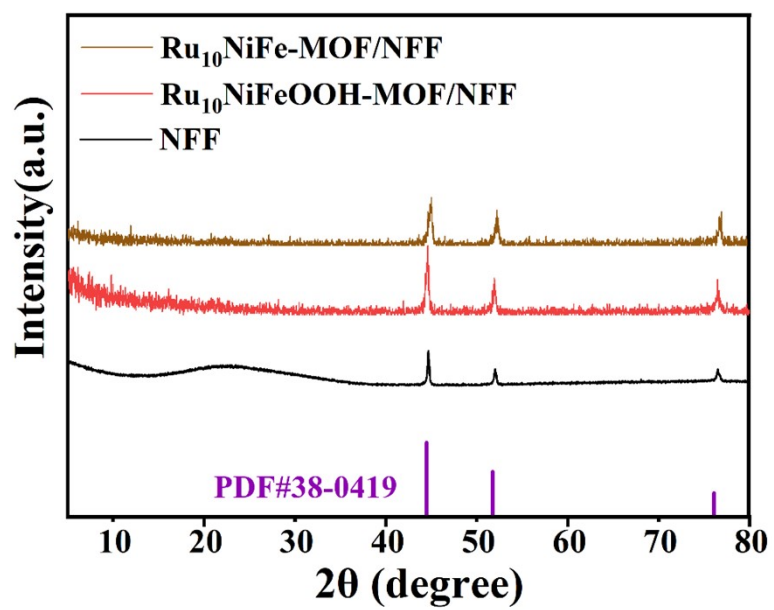


Fig.S4. XRD images of $\text{Ru}_{10}\text{NiFe-MOF/NFF}$, $\text{Ru}_{10}\text{NiFeOOH-MOF/NFF}$ and NFF.

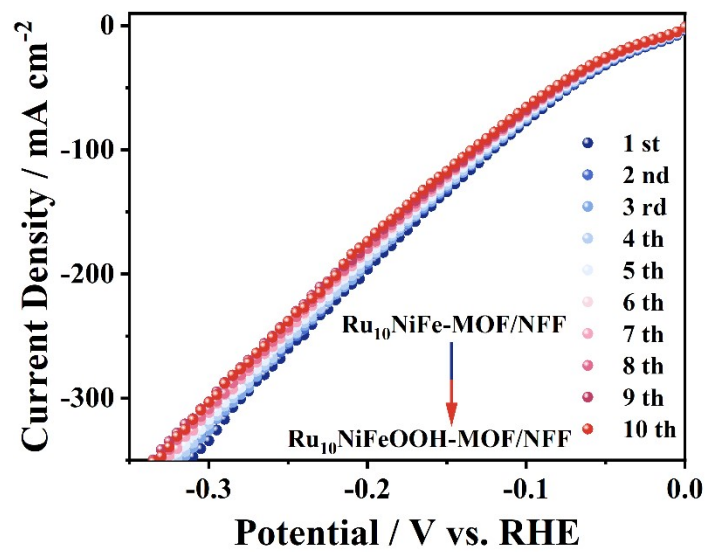


Fig.S5. Fast scan LSV map of 10 HER tests of Ru₁₀NiFe-MOF/NFF.

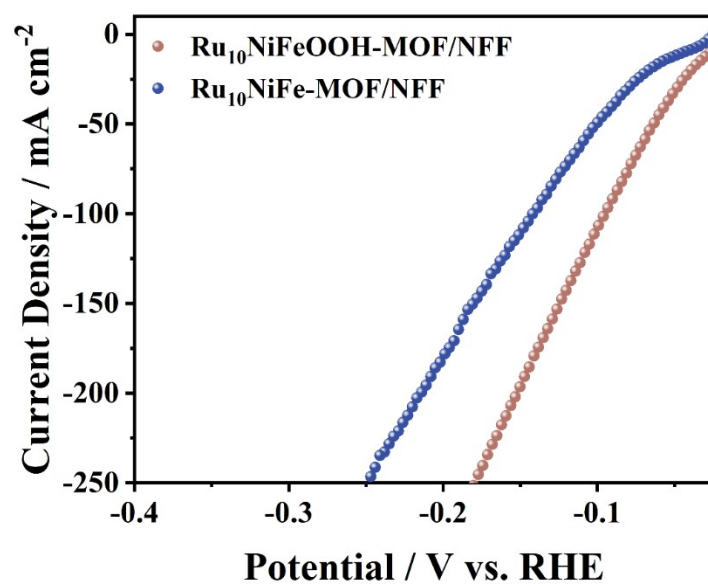


Fig.S6.LSV images of Ru₁₀NiFe-MOF/NFF and Ru₁₀NiFeOOH-MOF/NFF.

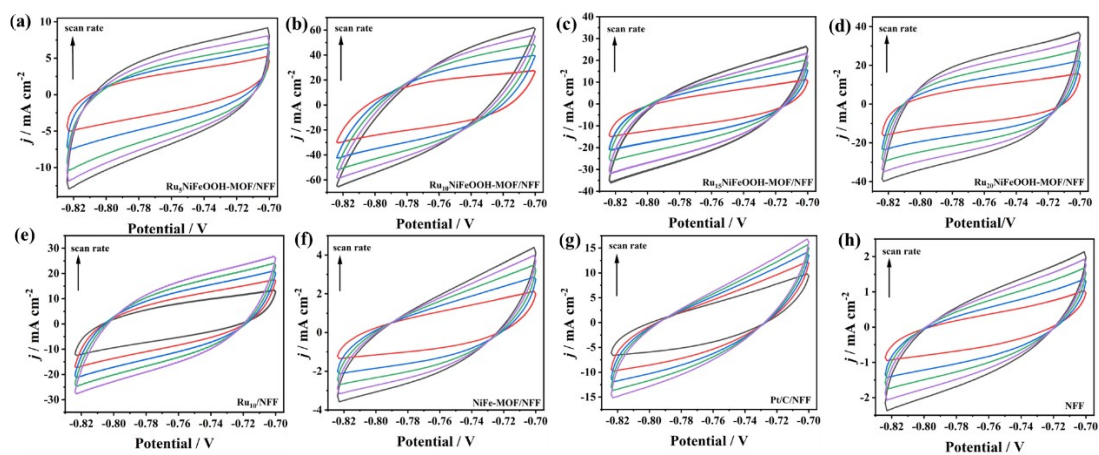


Fig.S7. (a-h) Cyclic voltammetry of $\text{Ru}_5\text{NiFeOOH-MOF/NFF}$, $\text{Ru}_{10}\text{NiFeOOH-MOF/NFF}$, $\text{Ru}_{15}\text{NiFeOOH-MOF/NFF}$, $\text{Ru}_{20}\text{NiFeOOH-MOF/NFF}$, $\text{Ru}_{10}/\text{NFF}$, NiFe-MOF/NFF , Pt/C/NFF , NFF at potentials of 0.02-0.1 V.

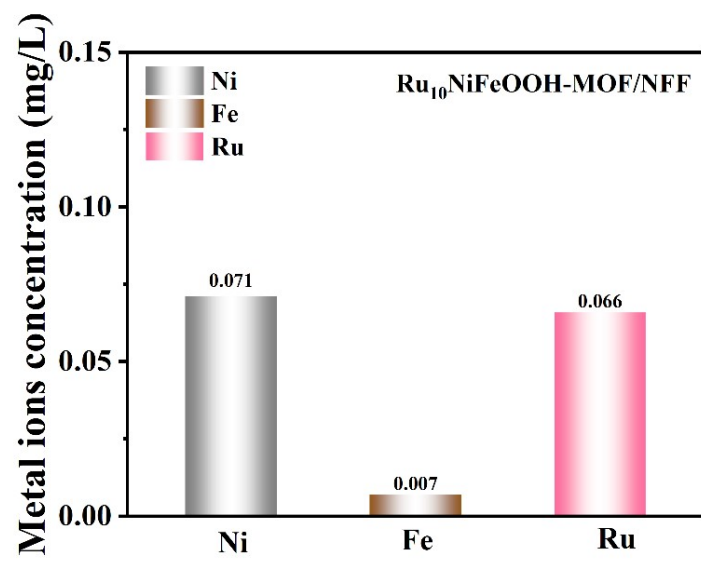


Fig.S8. ICP images of Ru₁₀NiFeOOH-MOF/NFF.

Tables

Table S1 Comparison of atomic percentages of different electrocatalysts

Sample	Element	Atomic percentage / %
Ru₅NiFe-MOF/NFF	C	53.18
	O	33.52
	Fe	5.64
	Ni	4.81
	Ru	2.84
Ru₁₀NiFe-MOF/NFF	C	51.89
	O	35.92
	Fe	5.79
	Ni	2.79
	Ru	3.62
Ru₁₅NiFe-MOF/NFF	C	54.31
	O	36.44
	Fe	6.41
	Ni	1.52
	Ru	1.32
Ru₂₀NiFe-MOF/NFF	C	60.27
	O	28.45
	Fe	6.11
	Ni	2.96
	Ru	2.21
Ru₁₀NiFeOOH-MOF/NFF	C	22.02
	O	47.35
	Fe	17.98
	Ni	3.55
	Ru	4.86

References

- [1] Kresse, G.; Furthmüller, J. Efficient Iterative Schemes for Ab Initio Total-Energy Calculations Using a Plane-Wave Basis Set. *Phys. Rev. B* 1996, 54, 11169–11186.
- [2] Perdew, J. P.; Burke, K.; Ernzerhof, M. Generalized Gradient Approximation Made Simple. *Phys. Rev. Lett.* 1996, 77, 3865–3868.
- [3] Kresse, G.; Joubert, D. From Ultrasoft Pseudopotentials to the Projector Augmented-Wave Method. *Phys. Rev. B* 1999, 59, 1758-1775.
- [4] Blöchl, P. E. Projector Augmented-Wave Method. *Phys. Rev. B* 1994, 50, 17953–17979.
- [5] Grimme, S.; Antony, J.; Ehrlich, S.; Krieg, H. *J. Chem. Phys.* 2010, 132, 154104.
- [6] Henkelman, G.; Uberuaga, B. P.; Jonsson, H. *J. Chem. Phys.* 2000, 113, 9901.